Hindawi
Advances in Civil Engineering
Volume 2019, Article ID 3453274, 13 pages
https://doi.org/10.1155/2019/3453274

Research Article

Flexural Capacity of Steel-Concrete Composite Beams under Hogging Moment

Jing Liu,[1,2] Fa-xing Ding,[1,3] Xue-mei Liu,[4] Zhi-wu Yu,[1] Zhe Tan,[2] and Jun-wen Huang[2]

[1]*School of Civil Engineering, Central South University, Changsha, Hunan Province 410075, China*
[2]*School of Civil Engineering, Hunan City University, Yiyang, Hunan Province 413000, China*
[3]*Engineering Technology Research Center for Prefabricated Construction Industrialization of Hunan Province, Changsha 410075, China*
[4]*Department of Infrastructure Engineering, The University of Melbourne, Parkville, VIC 3010, Australia*

Correspondence should be addressed to Fa-xing Ding; dinfaxin@csu.edu.cn

Received 14 October 2018; Revised 19 January 2019; Accepted 29 January 2019; Published 4 March 2019

Academic Editor: Robert Černý

This study investigates the flexural strength of simply supported steel-concrete composite beams under hogging moment. A total of 24 composite beams are included in the experiments, and ABAQUS software is used to establish finite element (FE) models that can simulate the mechanical properties of composite beams. In a parametric study, the influences of several major parameters, such as shear connection degree, stud arrangement and diameter, longitudinal and transverse reinforcement ratios, loading manner, and beam length, on flexural strength were investigated. Thereafter, three standards, namely, GB 50017, Eurocode 4, and BS 5950, were used to estimate the flexural strength of the composite beams. These codes were also compared with experimental and numerical results. Results indicate that GB 50017 may provide better estimations than the other two codes.

1. Introduction

Steel-concrete composite beams have been widely used in building construction. In engineering, situations occur in which composite beams undergo hogging bending. Examples of such situations include the following: (a) hogging bending regions near interior supports for continuous composite beams and (b) a beam is typically subjected to a hogging moment in areas near the column for a multistory frame structure.

Flexural capacity, which has become a major parameter due to its large cross section, has been widely applied in practice. Some studies have suggested that shear connection degree exerts a certain influence on flexural capacity, which can be theoretically divided into partial and full shear connections. The former reduces the stud number and benefits the colligation of reinforcing bars, whereas the latter guarantees bearing strength.

Therefore, various methods recommended by different codes have been proposed to estimate the flexural strength of composite beams. GB 50017 [1] presents a formula for calculating the flexural strength of the partial shear connection of composite beams in accordance with simplified plastic theory, which considers partial and full shear connections. BS 5950 [2] states that beams under hogging moment should be adequately anchored, and longitudinal reinforcement should be assumed to be stressed to its design strength $0.87f_y$, where it is in tension. The American Institute of Steel Construction (AISC)-Load Resistance Factor Design (LRFD) [3] and Eurocode 4 [4] rule that tension reinforcement should be adequately anchored and should be curtailed to suit the stud spacing in the negative moment regions of continuous beams. Experimental research and theoretical research on composite beams under hogging bending moment have been conducted in recent years. Some researchers have decided to study simply supported beams in the interest of simplicity.

Nie and Cai [5] considered the slips at the steel girder and concrete slab interface and then developed a model for predicting the mechanical behavior of composite beams under hogging moment. The finite element (FE) software, ANSYS, was also used. Amadio et al. [6] dealt with the

evaluation of the effective width of composite beams; the effective width increased with the load for all the test specimens. Loh et al. [7] studied the behavior of eight composite beams under hogging moment through an extensive experiment. Parameters, including reinforcement percentage and shear connection degree, were varied. Pecce et al. [8] conducted four experimental tests on simply supported composite beams under negative moment, in which the type, width, and connection degree were varied. Lin et al. [9, 10] studied the mechanical behavior of composite beams under negative bending moment through research test on fatigue and ultimate static loading. Vasdravellis et al. [11] presented a numerical and experimental study on steel-concrete composite beams subjected to the combined effects of negative or positive bending and axial compression.

FE modeling is a major analysis method for predicting the response of steel-concrete composite structures.

Zhu et al. [12] presented a numerical study on the property of studs and its application to steel-concrete composite beams. Chang et al. [13, 14] investigated the property of rock and composite structures through ABAQUS. Mirza and Uy [15] researched the mechanical behavior of composite beam-column flush end-plate connections subjected to high-consequence, low-probability loading via ABAQUS. Vasdravellis et al. [11] developed a nonlinear FE model to predict the nonlinear response of tested composite beams. The model relies on ABAQUS software. Li et al. [16] presented an FE modeling to investigate the behavior of concrete-filled steel tubular column-column connections. Zhao et al. [17] investigated the bearing capacity of a corroded reinforced concrete beam using ABAQUS.

The aforementioned literature indicates that steel-concrete composite beams generally perform well under flexural loadings. Some parameters, including shear connection degree, stud diameter, transverse and longitudinal reinforcement ratios, and loading condition, which influence the flexural strength of composite beams, have not been thoroughly investigated through experimental studies. Also, other factors, such as beam span, studs in double row layout, and loading manner and position, have not been discussed. Moreover, the standards of various countries have not been compared under a considerably wide range of factors that cover experimental and FE results.

Hence, the current study aims to make a thorough investigation on the flexural strength of steel-concrete composite beams and evaluating different methods for calculating flexural strength proposed in various standards. On the basis of the experimental, theoretical, and numerical research of our team [18–20], this study has four objectives: (1) to investigate the flexural capacity of 24 simply supported steel-concrete composite beams under hogging moment through an experimental study; (2) to simulate the flexural performance of the composite beams by establishing FE models using the ABAQUS program; (3) to investigate the effects of different factors on the flexural behavior of steel-concrete composite beams through parametric analysis; and (4) to evaluate different methods, including those of GB 50017, Eurocode 4, and BS 5950, with respect to the experimental and numerical results.

2. Experimental Study

2.1. Materials and Specimens. Ding et al. [19] conducted 22 simply supported steel-concrete composite beam experimental investigations on hysteretic behavior. In the current work, 24 steel-concrete composite beams, including SCB19-SCB20 (loading mode was monotonic), were included in the test study.

Figure 1 shows the cross section details of the girders. Figures 2 and 3 present the composite beam test loading device. Table 1 lists the geometric properties and characteristics of the composite beams. l is the specimen length, h_c is the concrete slab depth, w_c is the concrete slab width, h_s is the steel beam height, w_s is the steel beam width, and d is the stud diameter. ρ_{st} and ρ_{sl} are the transverse and longitudinal reinforcement ratios of the concrete slab, respectively. η is the degree of shear connection in the hogging moment region (based on GB 50017).

For convenient calculation and analysis, parameters related to the specimens in the literature (Lin et al. [9], Nie [21], and Vasdravellis et al. [11]) are also provided in Table 1. The maximum load per stud was investigated via a push-out test [11].

Table 2 presents the properties of steel and concrete. f_{cu} is the cubic compressive strength of concrete, $f_{s,b}$ is the yield strength of steel, $f_{s,s}$ is the yield strength of stud, $f_{s,r}$ is the yield strength of longitudinal reinforcement, and f_u is the ultimate strength of stud. Various concrete grades are included in the study with concrete strength varying from 35.5 MPa to 49.7 MPa. The tensile strengths of steel are ranging from 250 to 324 MPa as per design.

2.2. Testing System and Method. A total of 24 test specimens were designed and experimented using two approaches. The first approach adopted the monotonic loading mode and included two specimens labeled SCB19 and SCB20. The second approach applied the dynamic cyclic loading mode and included the remaining 22 specimens. The failure process and phenomenon of such beams can be found in the study of Ding et al. [18]. The experimental load-deflection curves of composite beams under dynamic cyclic loading are also described in that article.

2.3. Experimental Results and Discussion. Shear connection degree is a principal factor for the calculation of composite beams' flexural strength under various codes; therefore, its definition is presented here with the expression for the subsequent discussion:

$$\eta = \frac{n}{n_f}, \tag{1}$$

where n_f is the number of connectors for full shear connection, $n_f = V_s/V_u$. n is the actual number of studs between the adjacent support and the intermediate point. V_s is the entire horizontal shear at the interface between the concrete slab and the steel girder, $V_s = A_{st} f_{st}$, where A_{st} is the longitudinal reinforcement area and f_{st} is the yield strength of the longitudinal reinforce area. V_u is the nominal strength of a single stud shear connector. The definitions of V_s and V_u

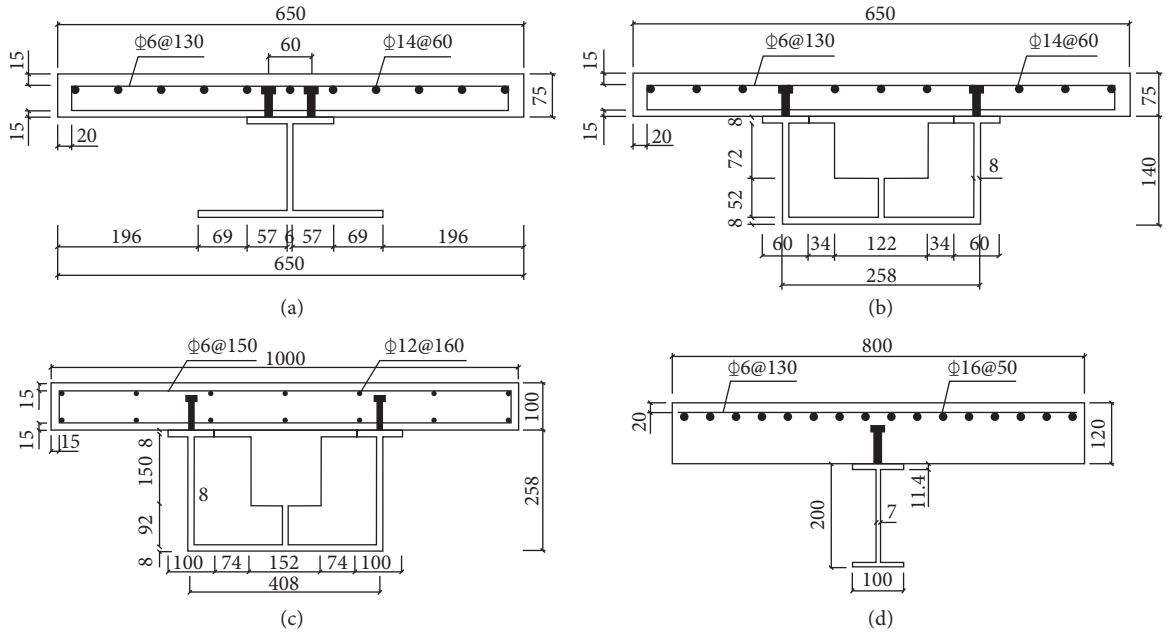

Figure 1: Cross section details of the girders: (a) SCB1~2, (b) SCB3~8, (c) SCB9~13, and (d) SCB14~24.

Figure 2: Test setup on the spot: (a) SCB1~2, (b) SCB3~8, (c) SCB9~13, and (d) SCB14~24.

may vary with the standards, including GB 50017, BS 5950, AISC-LRFD, and Eurocode 4.

To understand the factors that influence the flexural capacity of composite beams, this section focuses on discussing such factors.

2.3.1. Shear Connection Degree. Figure 4 shows the relationship between flexural strength and shear connection degree. The contrast of SCB3–SCB5, SCB11–SCB13, and SCB14–SCB18 illustrates that a higher shear connection degree leads to greater flexural strength. When η is high, the steel-concrete composite beams exhibit good interaction behavior, which can minimize the deflection of composite beams under loading and guarantee bearing capacity.

2.3.2. Ratio of Transverse Reinforcement. Figure 5 shows the relationship between transverse reinforcement ratio and flexural strength. The contrast of SCB21–SCB24 shows that the transverse reinforcement ratios of 0.20%–0.78% exert a certain influence on bearing strength. The capacity in the negative moment of SCB24 is 12.0% higher than that of SCB21. This result contributes to the higher transverse

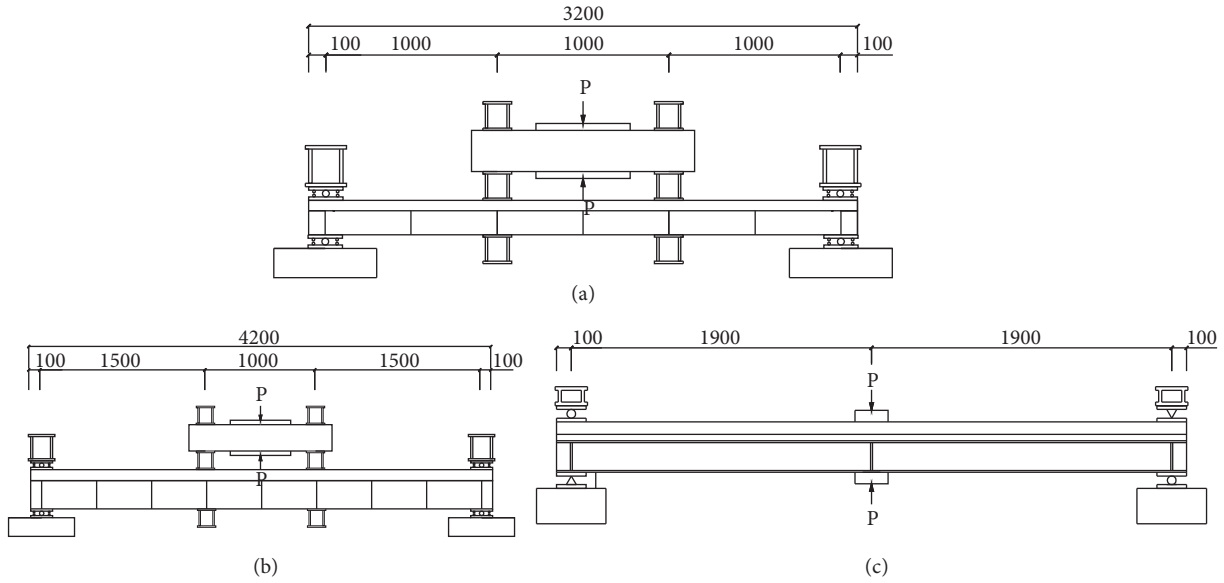

Figure 3: Experimental setup for all specimens: (a) SCB1~8, (b) SCB9~13, and (c) SCB14~24.

reinforcement ratio and exerts the confined effect, which ensures that the concrete slab, stud, and steel girder work better to improve the flexural capacity of composite beams.

2.3.3. Ratio of Longitudinal Reinforcement. Figure 6 illustrates the relationship between M and ρ_{sl}. The contrast of SCB3–SCB8 shows that the longitudinal reinforcement ratios of 1.89% or 3.47% exert an appreciable impact on limit bearing capacity. Flexural capacity increases with the longitudinal reinforcement ratio. This result contributes to the higher longitudinal reinforcement ratio that can participate in force, which improves the ultimate flexural strength of the composite beams in the negative moment region.

2.3.4. Diameter of Studs. Figure 7 illustrates the relationship between M and d. The diameters of the studs of SCB21–SCB23 are 13, 16, and 19 mm, respectively. These specimens have the same shear connection degree (approximately 2.5). The flexural capacity of SCB10 is 2.3% higher than that of SCB9, and the bearing capacity of SCB11 is 1.4% higher than that of SCB9, thereby indicating that bearing capacity is unaffected by stud diameter.

3. Methods for Estimating Flexural Capacity

3.1. GB 50017. In the Chinese national standard GB 50017, the flexural capacity M of composite beams under hogging moment is expressed as follows:

(1) When $\eta \geq 1$,

$$M = M_s + A_{st} f_{st} \left(\frac{y_3 + y_4}{2} \right), \tag{2}$$

$$M_s = (S_1 + S_2) f_y, \tag{3}$$

where S_1 = the area moment above the steel beam's neutral axis, S_2 = the area moment below the steel beam's neutral axis, y_3 = the distance between the longitudinal reinforcement's neutral axis to the composite beam neutral's axis, y_4 = the distance between the steel beam axis to the composite beam neutral axis, M_s = the flexural load capacity of the steel beams, and A_{st} = the longitudinal reinforce area in the effective width of the concrete slab.

V_u denotes the nominal strength of a single stud. It is defined as follows:

$$V_u = 0.43 k A_{sd} (f_c E_c)^{0.5} < 0.7 k A_{sd} f_u, \tag{4}$$

where A_{sd} = the cross-sectional area of the stud, E_c = Young's modulus of concrete, f_c = the compressive strength of concrete, $V_s = A_s f_s$, A_s = the cross-sectional area of steel, and A_c = is the cross-sectional area of concrete. For the negative moment, the shear bearing capacity of the studs should be multiplied by a folding coefficient k, where $k = 0.9$.

(2) When $\eta \leq 1$, the bending capacity is still in accordance with formula (2). $A_{st} f_{st}$ should be regarded as a smaller value of $A_{st} f_{st}$ and $n_r N_v$. n_r indicates the number of studs in the shear span.

3.2. BS 5950. For hogging moment, the longitudinal reinforcement is supposed to be stressed to its design strength of $0.87 f_y$, where it is in tension, and the beam should be adequately anchored.

3.3. Eurocode 4. Eurocode 4 and AISC–LRFD state that, in the negative moment regions, tension reinforcement should be curtailed to suit shear connector spacing and should be adequately anchored.

Table 1: Geometric properties and characteristics of composite beams.

Source of the specimens	No.	Loading mode	l (mm)	w_c (mm)	h_c (mm)	w_s (mm)	h_s (mm)	d (mm)	η	ρ_{st} (%)	ρ_{sl} (%)	M (kN)
This paper	SCB1	Dynamic cyclic	3000	650	75	258	140	13	1.44	0.62	3.47	120
	SCB2	Dynamic cyclic	3000	650	75	258	140	13	0.55	0.62	3.47	121
	SCB3	Dynamic cyclic	3000	650	75	258	140	13	1.44	0.62	3.47	158
	SCB4	Dynamic cyclic	3000	650	75	258	140	13	1	0.62	3.47	146
	SCB5	Dynamic cyclic	3000	650	75	258	140	13	0.55	0.62	3.47	132
	SCB6	Dynamic cyclic	3000	650	75	258	140	13	2.64	0.62	1.89	131
	SCB7	Dynamic cyclic	3000	650	75	258	140	13	1.83	0.62	1.89	123
	SCB8	Dynamic cyclic	3000	650	75	258	140	13	1.01	0.62	1.89	120
	SCB9	Dynamic cyclic	4000	1000	100	408	258	13	3.14	0.38	1.58	390
	SCB10	Dynamic cyclic	4000	1000	100	408	258	16	3.25	0.38	1.58	399
	SCB11	Dynamic cyclic	4000	1000	100	408	258	19	3.22	0.38	1.58	395
	SCB12	Dynamic cyclic	4000	1000	100	408	258	16	2.26	0.38	1.58	392
	SCB13	Dynamic cyclic	4000	1000	100	408	258	16	4.24	0.38	1.58	405
	SCB14	Dynamic cyclic	3800	800	120	100	200	16	1.83	0.32	2.51	207
	SCB15	Dynamic cyclic	3800	800	120	100	200	16	1.59	0.32	2.51	198
	SCB16	Dynamic cyclic	3800	800	120	100	200	16	1.3	0.32	2.51	193
	SCB17	Dynamic cyclic	3800	800	120	100	200	16	1.06	0.32	2.51	189
	SCB18	Dynamic cyclic	3800	800	120	100	200	16	0.83	0.32	2.51	187
	SCB19	Monotonic	3800	800	120	100	200	16	1.74	0.32	1.88	172
	SCB20	Monotonic	3800	800	120	100	200	16	2.22	0.32	1.47	165
	SCB21	Dynamic cyclic	3800	800	120	100	200	16	1.3	0.20	2.51	200
	SCB22	Dynamic cyclic	3800	800	120	100	200	16	1.3	0.43	2.51	211
	SCB23	Dynamic cyclic	3800	800	120	100	200	16	1.3	0.59	2.51	206
	SCB24	Dynamic cyclic	3800	800	120	100	200	16	1.3	0.78	2.51	224
Nie [21]	NSCB5	Monotonic	3840	800	125	100	200	16	4.62	0.60	0.88	132
	NSCB6	Monotonic	3840	800	125	100	200	16	3.05	0.60	1.33	144
	NSCB7	Monotonic	3840	800	125	100	200	16	2.60	0.60	1.55	175
	NSCB8	Monotonic	3840	800	125	100	200	16	2.02	0.60	2.01	183
Lin et al. [9]	LCB1	Monotonic	4000	800	250	400	641	22	1.79	1.06	1.98	3981
	LCB5	Monotonic	4000	800	250	400	641	22	1.79	1.06	1.98	4003
	LCB7	Monotonic	4000	800	250	400	641	22	1.51	1.06	1.98	3801
Vasdravellis et al. [11]	VCB1	Monotonic	4000	600	120	133.9	206.8	19	2.68	0.24	0.63	186

4. FE Analysis

4.1. FE Modeling

4.1.1. Material Constitutive Models. The material constitutive models of concrete and steel suggested by Ding et al. [18] are used for the model. The detailed parameters are provided in the study of Ding et al. [18].

The stiffness of the spring element is defined by load-slip curves and is used to simulate the shear stud. The formula proposed by Ding et al. [20] through a bidirectional push-off test can be used for concrete in tension.

The equation can be written as

$$y = \begin{cases} \dfrac{A_4 x + (B_4 - 1)x^2}{1 + (A_4 - 2)x + B_4 x^2}, & x \le 1, \\ \dfrac{x}{0.15(x-1)^2 + x}, & x > 1, \end{cases} \tag{5}$$

where $y = p/p_u$, $x = s/s_0$, and $B_4 = 1.6(A_4 - 1)2$. s_0 is the value of slip corresponding to the peak load, and $s_0 = 100/d$. The ascending parameter A_4 is defined as the ratio of bond stiffness to peak secant stiffness, and $A_4 = (10d - 80)/(0.7d - 5)$. p_u is the shear capacity per stud. For a slip up to 5 mm, V reaches 99% of the ultimate load V_u. When the longitudinal, lateral, and vertical stiffness adopt expression (5) in this paper, good results can be obtained.

4.1.2. Model Skills. FE models are established using the ABAQUS program [22], which is extensively adopted in analyzing rock and composite structures (Chang et al. [13, 14]). Steel beams are modeled by using four-node reduced integral format shell elements (S4R). Concrete is modeled by using eight-node brick elements (C3D8R). Reinforcement bars in the specimens are modeled by the truss element T3D2 because this truss element is effective and accurate in simulating reinforcement in steel-concrete composite beams according to Ding et al. [18].

Figure 8 shows the simplified FE models for steel-concrete composite beams. Spring and beam elements (B31) are used to model the studs, which can be seen in Figures 8(a) and 8(b), respectively. The model uses a structured meshing technique. The surface-to-surface and Coulomb friction model is defined as the type of contact between the steel girder and the concrete slab.

Table 2: Properties of steel and concrete.

No.	$f_{s,s}$ (MPa)	f_u (MPa)	$f_{s,b}$ (MPa)	$f_{s,r}$ (MPa)	f_{cu} (MPa)
SCB1	330	440	324	453	35.5
SCB2	330	440	324	453	35.5
SCB3	330	440	324	453	35.5
SCB4	330	440	324	453	35.5
SCB5	330	440	324	453	35.5
SCB6	330	440	324	453	35.5
SCB7	330	440	324	453	35.5
SCB8	330	440	324	453	35.5
SCB9	330	440	320	440	43.7
SCB10	350	460	320	440	43.7
SCB11	350	455	320	440	43.7
SCB12	350	460	320	440	43.7
SCB13	350	460	320	440	43.7
SCB14	350	480	250	380	44.3
SCB15	350	480	250	380	44.3
SCB16	350	480	250	380	43.4
SCB17	350	480	250	380	48.5
SCB18	350	480	250	380	42.2
SCB19	350	480	250	380	38.2
SCB20	350	480	250	380	46.2
SCB21	350	480	320	380	41.9
SCB22	350	480	320	380	42.1
SCB23	350	480	320	380	49.7
SCB24	350	480	320	380	40.8
NSCB5	417	535	394	389	36
NSCB6	417	535	394	389	38.2
NSCB7	417	535	394	389	27.4
NSCB8	—	—	370	510	21
CB1	417	535	394	389	36
CB5	417	535	394	389	38.2
CB7	417	535	394	389	27.4
CB1	—	—	370	510	21

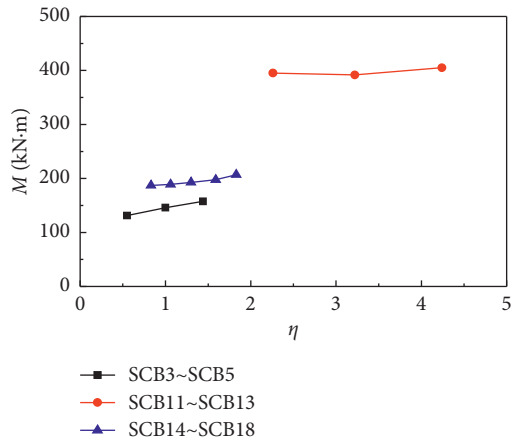

Figure 4: Relationship between M and η.

4.2. Flexural Capacity from FE Analysis (FEA). Figure 9 shows the comparison between the calculated and tested load-deformation curves of a composite beam. Figure 10 illustrates the comparison between the calculated and tested load-end slips of a composite beam. Figure 11 demonstrates the comparison between the calculated and tested longitudinal reinforcement and bottom flange strains of a composite beam.

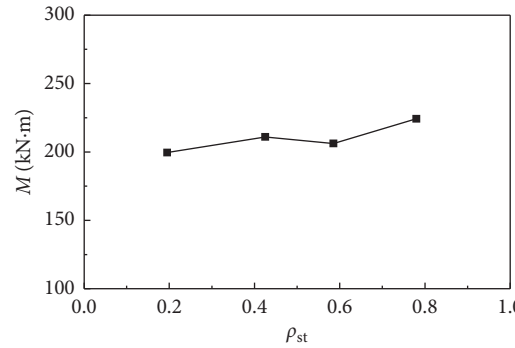

Figure 5: Relationship between M and ρ_{st}.

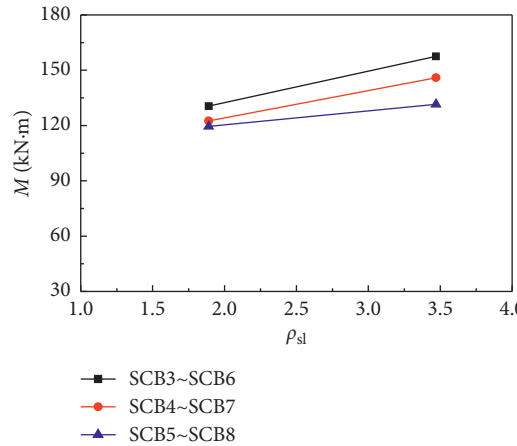

Figure 6: Relationship between M and ρ_{sl}.

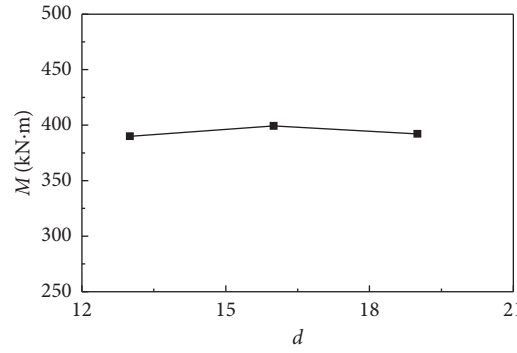

Figure 7: Relationship between M and d.

Good agreement between FEA and the measured results is found in the elastic stage. Thereafter, the curve from the calculated and test results appeared with a certain deviation in the elastic-plastic and failure stages.

Table 3 presents the comparison between the simulated and test results. A total of 32 groups of test data regarding steel-concrete composite beams are included for analysis and model validation. M is the measured values of flexural capacity, M_{11} is the flexural strength obtained via the spring element modeling method, and M_{12} is the flexural strength obtained via the beam element modeling method. M_2, M_3, and M_4 are the flexural capacities under GB 50017, BS 5950,

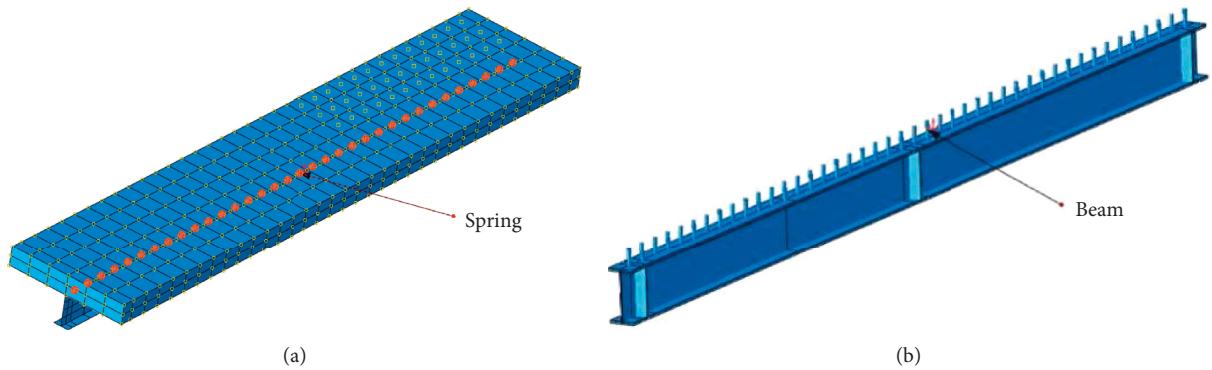

Figure 8: Simplified FE models for steel-concrete composite beams. (a) Spring elements for studs and (b) beam elements for studs.

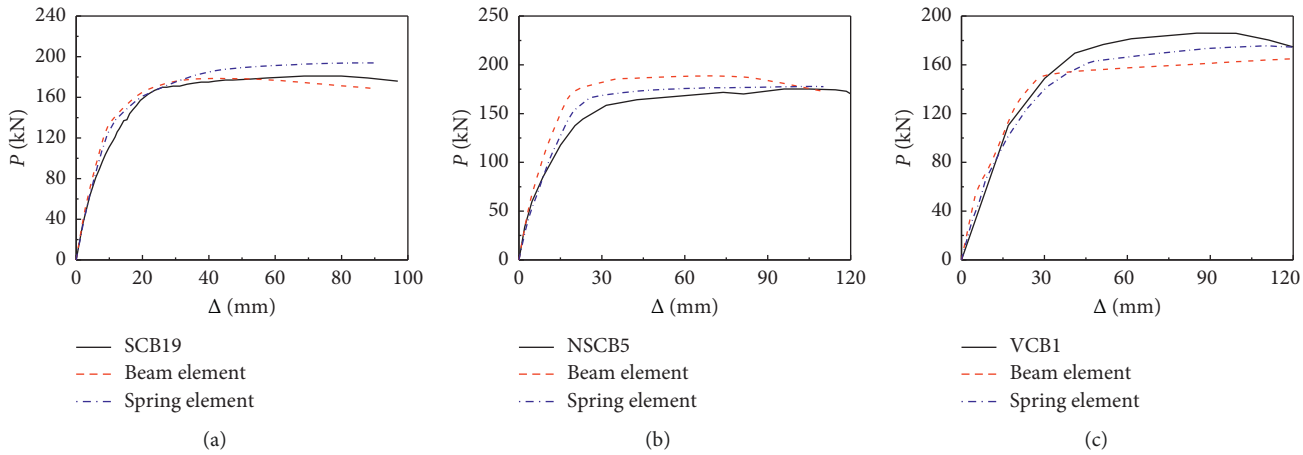

Figure 9: Comparison between the calculated and tested load-deformation curves of a composite beam. (a) SCB19 (present study), (b) NSCB5 (Nie and Cai [5]), and (c) VCB1 (Vasdravellis et al. [11]).

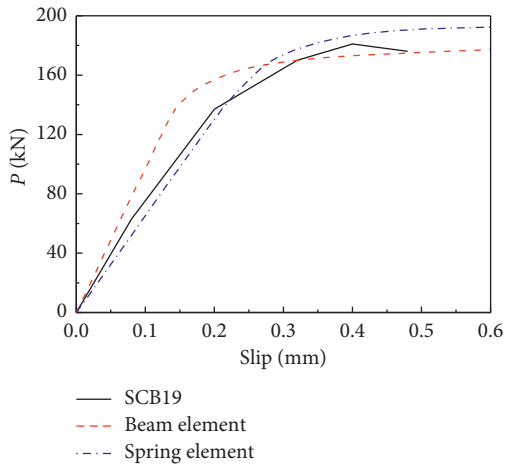

Figure 10: Comparison between the calculated and tested load-end slips of a composite beam.

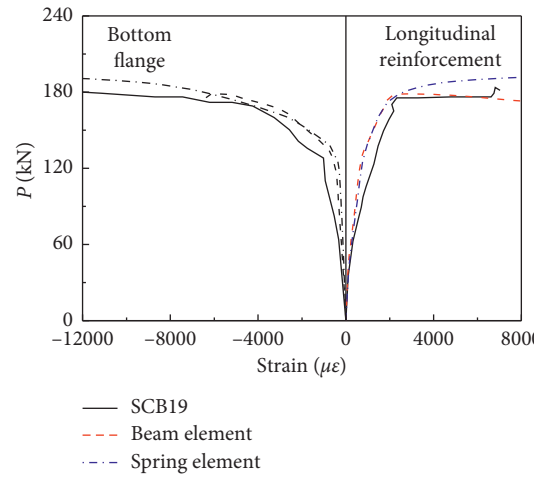

Figure 11: Comparison between the calculated and tested longitudinal reinforcement and bottom flange strains of a composite beam.

and Eurocode 4, respectively. The test results are compared using different methods, including FEA and three standards.

The average M/M_{11} ratio is 1.026 with a coefficient of variation at 0.073 for the spring element, and the average M/M_{12} ratio is 0.963 with a coefficient of variation at 0.085 for the beam element. Such findings indicate that the FE simulation results are extremely close to the test results.

4.3. Parametric Study. Parameter analysis is conducted in this section. In addition, a comparison study is also performed between the FEA results and the standard results. The spring element is used for FEA in the subsequent study, given the following reasons. First, the spring element method exhibits faster computational speed. Second, the spring element can

Table 3: Comparison among the three standards and simulated and test results.

No.	Source of the specimens	Total number of specimens	Characteristic value	Spring element M/M_{11}	Beam element M/M_{12}	GB 50017 M/M_2	BS 5950 M/M_3	Eurocode 4 M/M_4
1	This paper	24	Average	1.037	0.981	1.031	1.161	1.049
			Coefficient of variation	0.063	0.093	0.058	0.151	0.065
2	Nie [21]	4	Average	0.993	0.932	1.098	1.195	1.060
			Coefficient of variation	0.091	0.034	0.061	0.067	0.064
3	Lin et al. [9]	3	Average	1.000	0.962	1.169	1.306	1.073
			Coefficient of variation	0.104	0.088	0.031	0.032	0.033
4	Vasdravellis et al. [11]	1	Average	1.099	0.863	1.208	1.348	1.083
			Coefficient of variation	—	—	—	—	—
5	All above	32	Average	1.026	0.963	1.058	1.185	1.036
			Coefficient of variation	0.073	0.085	0.073	0.140	0.088

accurately simulate the stud stiffness value in each direction, which is important for the simulation because stud stiffness reflects stud mechanical properties.

4.3.1. Influence of Shear Connection Degree. Figure 12 shows the geometric properties of a composite beam that is loaded at midspan. Steel-concrete composite beam depth-span ratio, steel girder section size, and concrete slab size are according to the specifications in GB 50017. The span is 12 m, the stud diameter is 19 mm, and its yield strength and limit strength are 350 MPa and 455 MPa, respectively. The studs are arranged in a single row layout. The steel-concrete composite beam models have six types of material combination groups: (1) C30 and C40 concrete paired with Q235 steel, (2) C40 and C50 concrete paired with Q345 steel, and (3) C50 and C60 concrete paired with Q420 steel. In total, 43 cases are available for study.

Figure 13 shows the M-ç relationship, which is also obtained from three methods. GB 50017, BS 5950, and Eurocode 4 are compared with the FEA results. The results show that shear connection degree exerts a marked impact on the flexural strength of composite beams. M is increased with the ç value. However, this phenomenon is not evident when ç is more than 1.

4.3.2. Influences of Other Factors

(1) Studs in Double Row Layout. In this research, stud diameter, loading position and manner, longitudinal reinforcement ratio, beam span, and section size are the same as those shown in Section 4.1. Two groups of composite beams are tested. The first group uses C30 concrete and Q235 steel, whereas the second group uses C50 concrete and Q420 steel. Figure 14 illustrates the influence of a double row layout for studs on M-ç relationship. The double row stud arrangement exerts minimal impact on the flexural strength of composite beams. The M-ç relationships of the composite beam with C30 concrete and Q235 steel obtained from GB 50017, Eurocode 4, and BS 5950, which are also compared with the FEA results, are shown in Figure 14.

(2) Stud Diameter. In this research, the number of shear studs per row across the flange, loading position and manner, longitudinal reinforcement ratio, beam span, and section size are the same as those shown in Section 4.1. One group of composite beams that use C40 concrete and Q345 steel is tested. The stud diameters are 13, 16, and 22 mm, respectively. Figure 15 illustrates the influence of stud diameter on M-ç relationship. Stud diameter exerts minimal impact on the flexural strength of composite beams. The M-ç relationships of the composite beam with C40 concrete and Q345 steel obtained from GB 50017, Eurocode 4, and BS 5950, which are also compared with the FEA results, are shown in Figure 15.

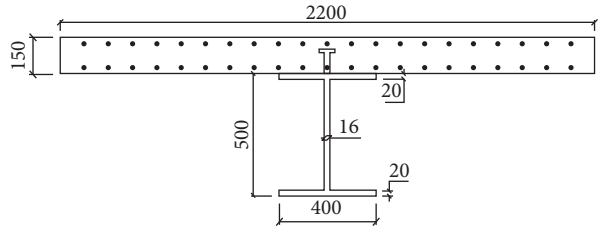

Figure 12: Geometric properties of a steel-concrete composite beam.

(3) Loading Position and Manner. In this research, the number of shear studs per row across the flange, stud diameter, longitudinal reinforcement ratio, beam span, and section size are the same as those shown in Section 4.1. Two groups of composite beams are studied. One group uses C30 concrete and Q235 steel, and the other group uses C50 concrete and Q420 steel. The loading positions are 1/4, 1/3, and 5/12 of the beam span. Figure 16 shows the influences of loading position and manner on M-ç relationship. Loading position and manner exert minimal impacts on the flexural strength of composite beams. The relationships between M and ç under the three types of methods are selected from the C30 and Q235 sample. The M-ç relationships of the composite beam with C30 concrete and Q235 steel obtained from GB 50017, Eurocode 4, and BS 5950 are also shown in Figure 16 and compared with the FEA results.

(4) Longitudinal Reinforcement Ratio. In this research, the number of shear studs per row across the flange, stud diameter, loading position and manner, beam span, and section size are the same as those shown in Section 4.1. One group of

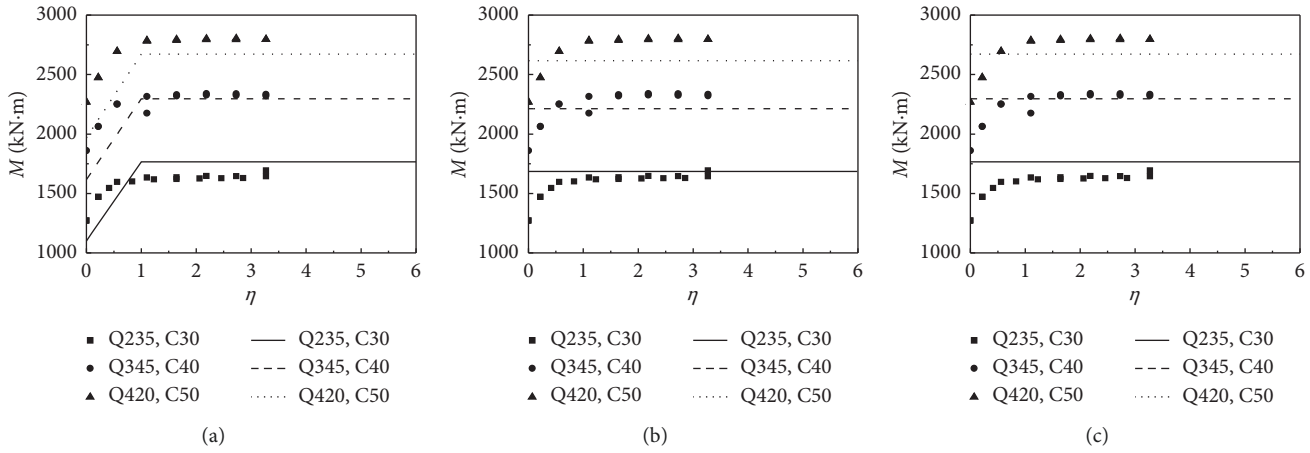

Figure 13: *M*-ç relationships: comparison between the results of (a) GB 50017 and FEA, (b) BS 5950 and FEA, and (c) Eurocode 4 and FEA.

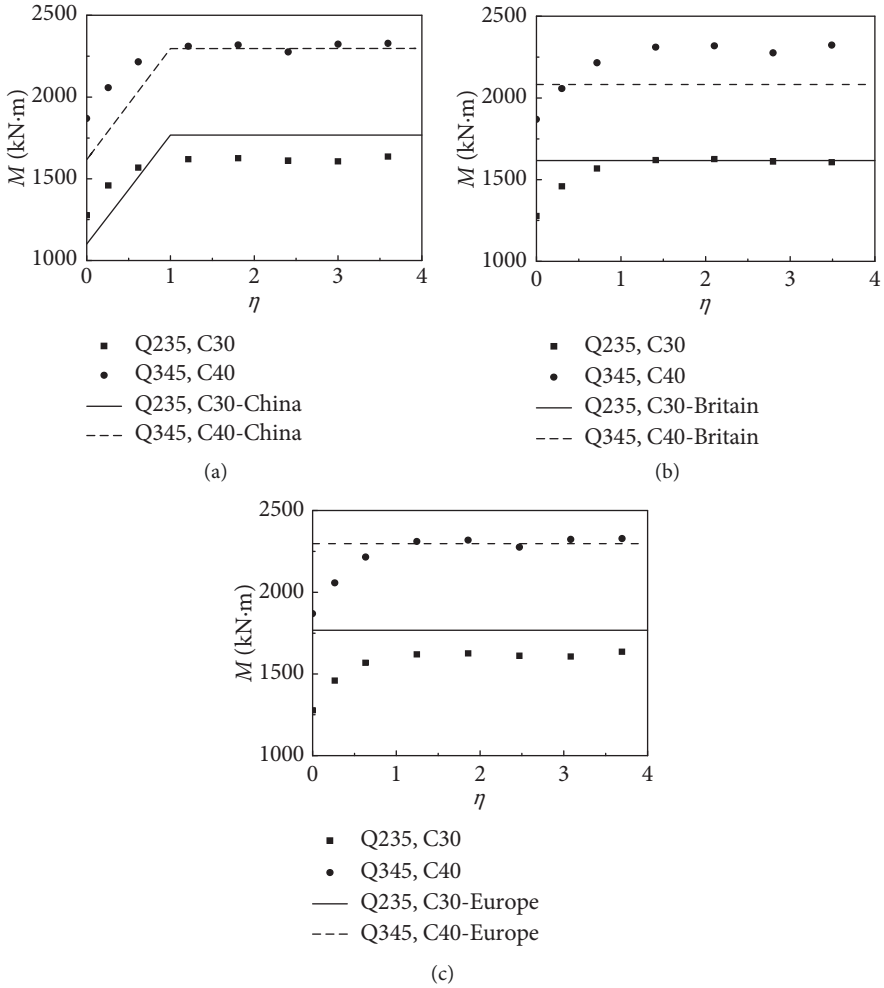

Figure 14: Influence of the double row stud layout on *M*-ç relationship: comparison between the results of (a) GB 50017 and FEA, (b) BS 5950 and FEA, and (c) Eurocode 4 and FEA.

composite beams (with C30 concrete and Q235 steel) is studied. The longitudinal reinforcement ratios are 0.38%, 1.28%, and 5.15%. Figure 17 illustrates the influence of the longitudinal reinforcement ratio on *M*-ç relationship. The longitudinal reinforcement ratio exerts a certain impact on the flexural strength of composite beams; that is, *M* is increased with the longitudinal reinforcement ratio at ç. The *M*-ç relationships of the composite beam with C40 concrete and Q345 steel obtained from GB 50017, Eurocode 4, and BS 5950, which are also compared with the FEA results, are shown in Figure 17.

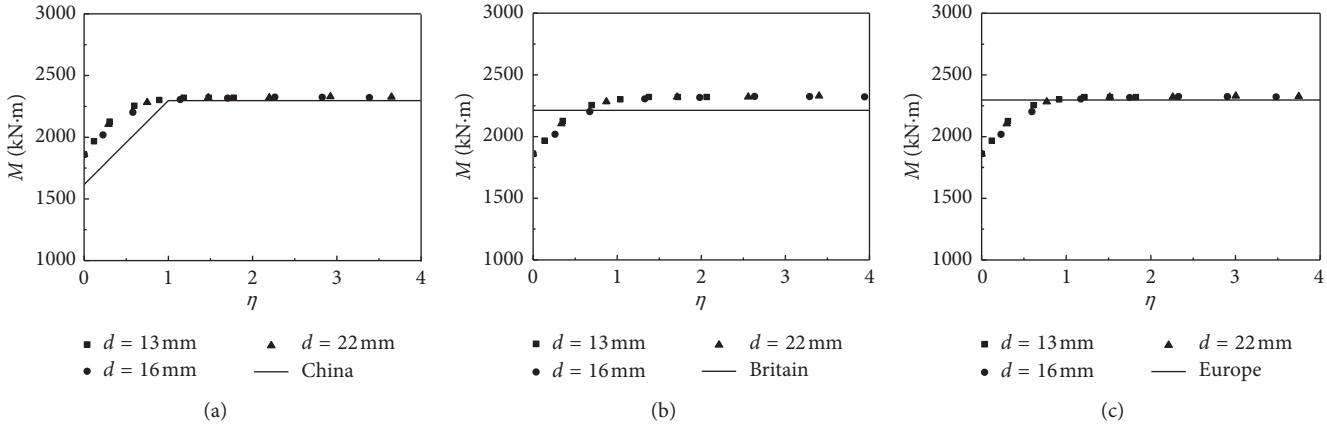

Figure 15: Influence of the stud diameter on M-$ç$ relationship: comparison between the results of (a) GB 50017 and FEA, (b) BS 5950 and FEA, and (c) Eurocode 4 and FEA.

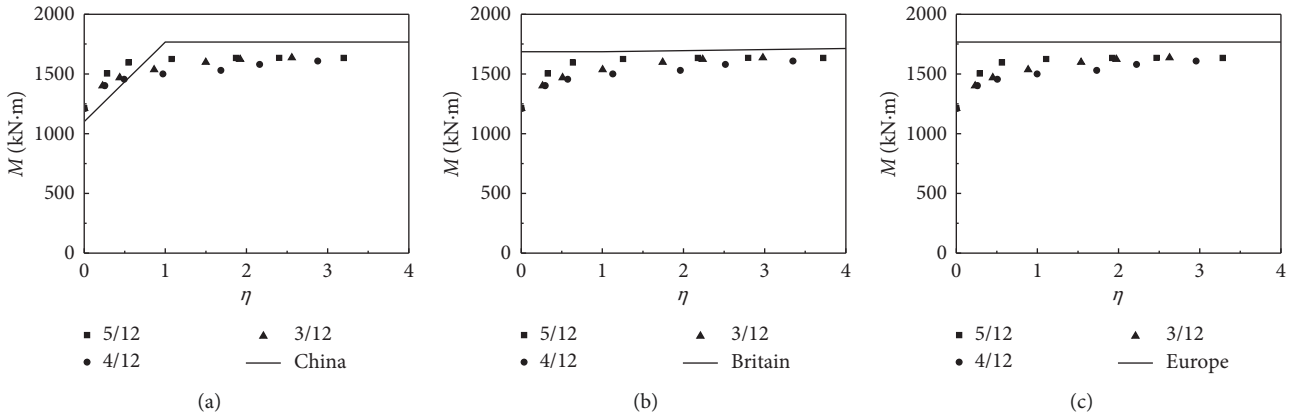

Figure 16: Influences of the loading position and manner on M-$ç$ relationship: comparison between the results of (a) GB 50017 and FEA, (b) BS 5950 and FEA, and (c) Eurocode 4 and FEA.

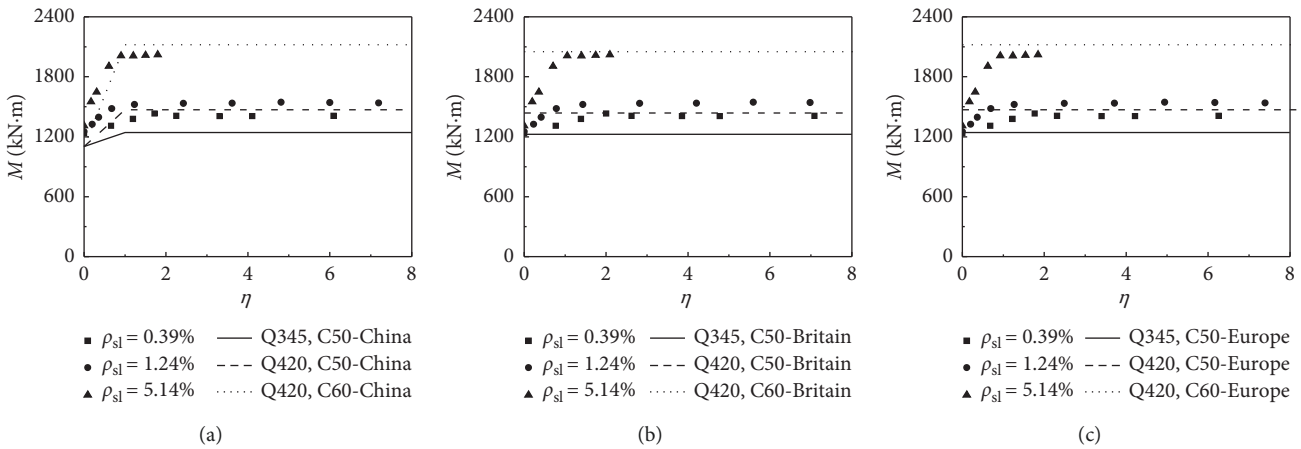

Figure 17: Influence of the longitudinal reinforcement ratio on M-$ç$ relationship: comparison between the results of (a) GB 50017 and FEA, (b) BS 5950 and FEA, and (c) Eurocode 4 and FEA.

(5) Span. In this research, the number of shear studs per row across the flange, stud diameter, loading position and manner, and longitudinal reinforcement ratio are the same as those shown in Section 4.1. Two groups of composite beams are studied. One group uses C40 concrete and Q235 steel, whereas the other group uses Q345 steel and C40 concrete. The span ranges from 4 m to 20 m. Figures 18(a)–18(d) show the influence of beam length on

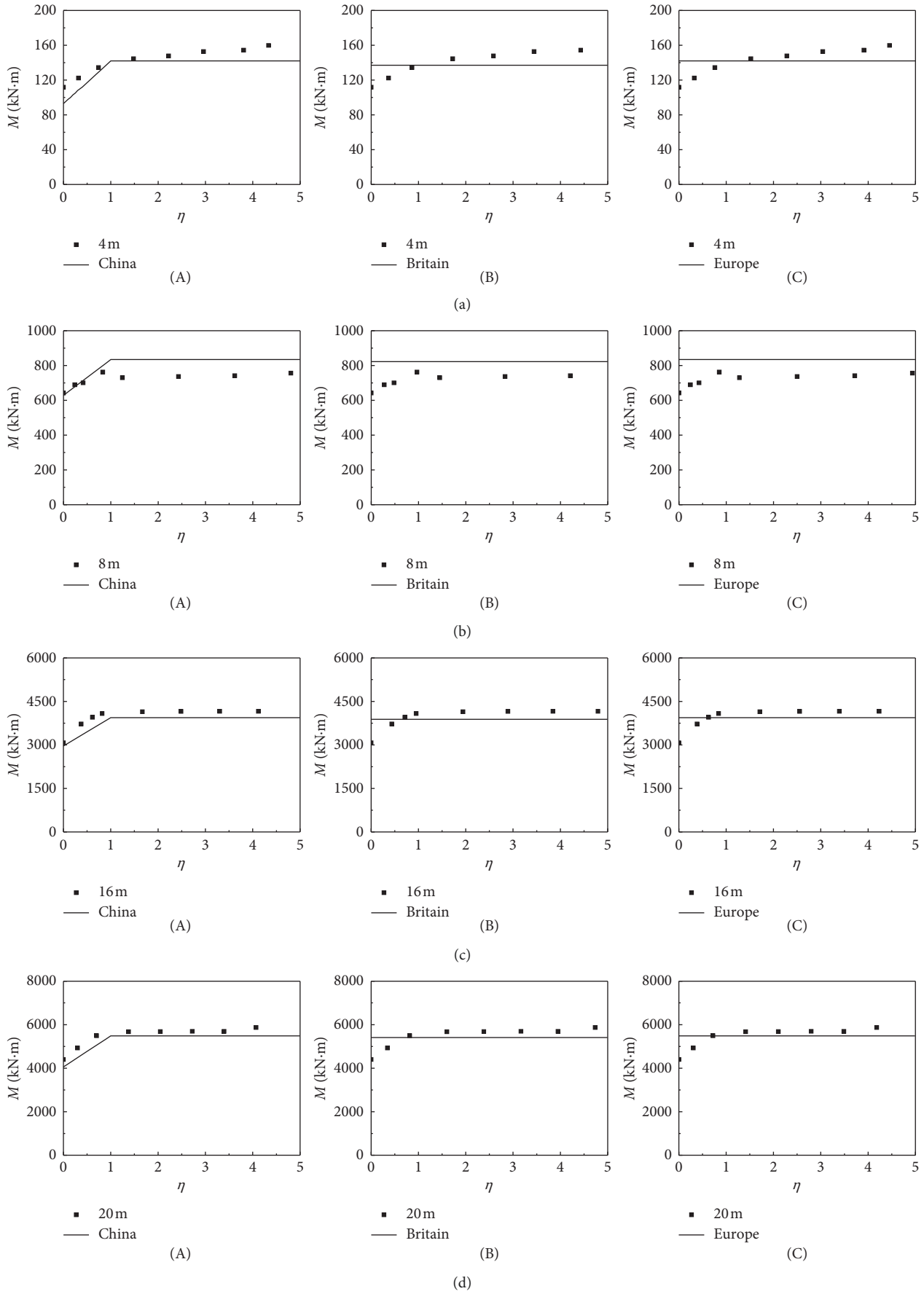

Figure 18: Influence of the beam length on M-φ relationship: comparison between the results of (A) GB 50017 and FEA, (B) BS 5950 and FEA, and (C) Eurocode 4 and FEA. (a) $l = 4$ m. (b) $l = 8$ m. (c) $l = 16$ m. (d) $l = 20$ m.

Table 4: Parameters of a steel-concrete composite beam.

l (m)	h_c (m)	b_c (m)	h_s (m)	w_s (m)	d (mm)	$f_{s,s}$ (MPa)	f_u (MPa)	f_{cu} (MPa)	f_{rl} (MPa)	$f_{s,b}$ (MPa)	ρ_{sl} (%)
4	0.08	0.8	0.2	0.1	16	350	455	C40	350	235, 345	1.88
8	0.12	1.5	0.4	0.25	19	350	455	C40	350	235, 345	2.23
12	0.15	2.2	0.5	0.4	19	350	455	C30, C40, C50, C60	350	235, 345, 420	2.56
16	0.16	2.4	0.75	0.45	22	350	455	C40	350	235, 345	2.72
20	0.20	2.6	0.9	0.5	22	350	455	C40	350	235, 345	2.54

Table 5: Comparison between the results of the three standards and the FE results.

No.	Type	Total number of specimens	Characteristic value	GB 50017 M_{FE}/M_2	BS 5950 M_{FE}/M_3	Eurocode 4 M_{FE}/M_4
1	Material	50	Average	1.048	1.048	0.949
			Coefficient of variation	0.087	0.097	0.087
2	Row of stud	16	Average	0.996	1.011	0.920
			Coefficient of variation	0.080	0.092	0.085
3	Diameter of stud	24	Average	1.039	1.061	0.962
			Coefficient of variation	0.049	0.079	0.075
4	Load pattern	21	Average	1.000	0.927	0.848
			Coefficient of variation	0.104	0.093	0.089
5	Span	32	Average	1.041	1.065	0.955
			Coefficient of variation	0.074	0.111	0.104
6	Longitudinal ratio	27	Average	1.097	1.097	0.992
			Coefficient of variation	0.069	0.152	0.134
7	Total	170	Average	1.043	1.044	0.945
			Coefficient of variation	0.084	0.117	0.106

M-$ç$ relationship. M is increased with the $ç$ value at different beam spans. The M-$ç$ relationships of the composite beam with C40 concrete and Q345 steel obtained from GB 50017, Eurocode 4, and BS 5950, which are also compared with the FEA results, are presented in Figure 18.

The parameters of a composite beam considered in the parametric study include steel strength from Q235 to Q420, concrete strength from C30 to C60, stud row layout (single or double), stud yield strength, limit strength from 350 MPa to 455 MPa, beam span from 4 m to 20 m, stud diameter from 16 mm to 25 mm, shear span ratio from 1/4 to 1/2, and load manner (point loading or uniformly distributed loading). Table 4 provides the parameters of a steel-concrete composite beam.

4.3.3. Summary and Discussion. Table 3 shows the comparison between the test results and those of the three standards (GB 50017, BS 5950, and Eurocode 4). The average M/M_2 ratio is 1.058 with a coefficient of variation at 0.073 for GB 50017. The average M/M_3 ratio is 1.185 with a coefficient of variation at 0.140 for BS 5950. The average M/M_4 ratio is 1.095 with a coefficient of variation at 0.086 for Eurocode 4.

Table 5 shows the comparison between the test results and those of the three standards. M_{FE} is the measured values of flexural capacity using ABAQUS. The shear connection degree is generally larger than 0.5 in practice; therefore, a shear connection degree that is smaller than 0.5 is not considered in the validation. The average M_{FE}/M_2 ratio is 1.043 with a coefficient of variation at 0.084. The average M_{FE}/M_3 ratio is 1.044 with a coefficient of variation at 0.117. The average M_{FE}/M_4 ratio is 0.945 with a coefficient of variation at 0.106.

Therefore, the calculation method of GB 50017 achieves higher accuracy than the other two standards.

5. Conclusions

This study explores and discusses the flexural strength of steel-concrete composite beams subjected to hogging moment through experimental and numerical studies, and then the results are compared with current widely used standard methods. The following conclusions can be obtained:

(1) The test results suggest that the higher the connection degree, the greater the flexural strength. The flexural strength increases with the transverse and longitudinal reinforcement ratios. The stud diameter and loading condition slightly affect flexural capacity.

(2) The stud can be simulated well using the beam and spring elements, and the calculated results achieve good agreement with the experimental results. In addition, compared with the beam element method, the spring element method exhibits faster computational speed and higher accuracy.

(3) On the basis of FEA with the spring element, the flexural capacity connection degree and longitudinal reinforcement ratio are identified as primary control factors. The larger the degree of shear connection, the greater the flexural strength. In addition, the growth of flexural capacity is insignificant when the shear connection degree reaches 1. Other factors, including loading location and manner, beam span,

stud diameter, and studs in double row layout, exert minimal impact on flexural capacity.

(4) Through experimental research and parametric analysis, the three calculation methods for flexural strength of composite beams are compared. The results show that China's specification may provide better estimations than the other two standard methods.

Data Availability

The data used to support the findings of this study are available from the corresponding author upon request.

Conflicts of Interest

The authors declare that they have no conflicts of interest.

Acknowledgments

This research work was financially supported by the National Key Research Program of China, Grant no. 2017YFC0703404, the China Postdoctoral Science Foundation Funded Project, Grant no. 2018M632990, the Natural Science Foundation of Hunan Province, China, Grant no. 2018JJ3021, and the Science and Technology Program of Yi Yang, Grant no. 2017YZ02.

References

[1] GB 50017-2017, *Standard for Design of Steel Structure*, China Architecture and Building Press, Beijing, China, 2017.

[2] BS 5950-3.1 British Standard, *Structural Use of Steelwork in Building. Part 3: Design in Composite Construction*, British Standards Institution, London, UK, 1994.

[3] AISC-LRFD, *Load and Resistance Factor Design Specification for Structural Steel Buildings*, American Institute of Steel Construction (AISC), Chicago, IL, USA, 2nd edition, 2005.

[4] EN 1994-1-1: Eurocode 4, "Design of composite steel and concrete structures," in *Part 1.1: General Rules and Rules for Buildings-General Rules*, European Committee for Standardization, Brussels, Belgium, 2004.

[5] J. Nie and C. S. Cai, "Steel-concrete composite beams considering shear slip effects," *Journal of Structural Engineering*, vol. 129, no. 4, pp. 495–506, 2003.

[6] C. Amadio, C. Fedrigo, M. Fragiacomo, and L. Macorini, "Experimental evaluation of effective width in steel-concrete composite beams," *Journal of Constructional Steel Research*, vol. 60, no. 2, pp. 199–220, 2004.

[7] H. Y. Loh, B. Uy, and M. A. Bradford, "The effects of partial shear connection in the hogging moment regions of composite beams," *Journal of Constructional Steel Research*, vol. 60, no. 6, pp. 897–919, 2004.

[8] M. Pecce, F. Rossi, F. A. Bibbo, and F. Ceroni, "Experimental behaviour of composite beams subjected to a hogging moment," *Steel and Composite Structures*, vol. 12, no. 5, pp. 395–412, 2012.

[9] W. Lin, T. Yoda, N. Taniguchi, H. Kasano, and J. He, "Mechanical performance of steel–concrete composite beams subjected to a hogging moment," *Journal of Structural Engineering*, vol. 140, no. 1, article 04013031, 2014.

[10] W. Lin, T. Yoda, and N. Taniguchi, "Application of SFRC in steel-concrete composite beams subjected to hogging moment," *Journal of Constructional Steel Research*, vol. 101, no. 1, pp. 175–183, 2014.

[11] G. Vasdravellis, B. Uy, E. L. Tan, and B. Kirkland, "Behaviour and design of composite beams subjected to negative bending and compression," *Journal of Constructional Steel Research*, vol. 79, no. 12, pp. 34–47, 2012.

[12] Z.-H. Zhu, L. Zhang, Y. Bai, F.-X. Ding, J. Liu, and Z. Zhou, "Mechanical performance of shear studs and application in steel-concrete composite beams," *Journal of Central South University*, vol. 23, no. 10, pp. 2676–2687, 2016.

[13] X. Chang, X. Luo, C. Zhu, and C. Tang, "Analysis of circular concrete-filled steel tube (CFT) support in high ground stress conditions," *Tunnelling and Underground Space Technology*, vol. 43, no. 7, pp. 41–48, 2014.

[14] X. Chang, J. Wang, C. Tang, and Z. Ru, "Effects of interface behavior on fracture spacing in layered rock," *Rock Mechanics and Rock Engineering*, vol. 49, no. 5, pp. 1733–1746, 2016.

[15] O. Mirza and B. Uy, "Behaviour of composite beam-column flush end-plate connections subjected to low-probability, high-consequence loading," *Engineering Structures*, vol. 33, no. 2, pp. 647–662, 2011.

[16] D. Li, B. Uy, V. Patel, and F. Aslani, "Behaviour and design of demountable CFST column-column connections subjected to compression," *Journal of Constructional Steel Research*, vol. 141, no. 2, pp. 262–274, 2018.

[17] S. A. Mirza, "Examination of strength modeling reliability of physical tests on structural concrete columns," *Advances in Civil Engineering*, vol. 2011, Article ID 428367, 16 pages, 2018.

[18] F. Ding, X. Ying, L. Zhou, and Z. Yu, "Unified calculation method and its application in determining the uniaxial mechanical properties of concrete," *Frontiers of Architecture and Civil Engineering in China*, vol. 5, no. 3, pp. 381–393, 2011.

[19] F.-X. Ding, J. Liu, X.-M. Liu, Z.-W. Yu, and Y.-S. Li, "Experimental investigation on hysteretic behavior of simply supported steel-concrete composite beam," *Journal of Constructional Steel Research*, vol. 144, no. 5, pp. 153–165, 2018.

[20] F.-X. Ding, G.-A. Yin, H.-B. Wang, L. Wang, and Q. Guo, "Static behavior of stud connectors in bi-direction push-off tests," *Thin-Walled Structures*, vol. 120, no. 11, pp. 307–318, 2017.

[21] J.-G. Nie, *Test, Theory and Application of Steel-Concrete Composite Beam*, Science Press, Beijing, China, 2005.

[22] K. Hibbitt and Sorensen Inc., *ABAQUS/Standard User's Manual, Version 6.8.,* Simulia Corp., Pawtucket, RI, USA, 2012.